

Atmospheric turbulence-induced signal fades on optical heterodyne communication links

Kim A. Winick

The three basic atmospheric propagation effects, absorption, scattering, and turbulence, are reviewed. A simulation approach is then developed to determine signal fade probability distributions on heterodyne-detected satellite links which operate through naturally occurring atmospheric turbulence. The calculations are performed on both angle-tracked and nonangle-tracked downlinks, and on uplinks, with and without adaptive optics. Turbulence-induced degradations in communication performance are determined using signal fade probability distributions, and it is shown that the average signal fade can be a poor measure of the performance degradation.

I. Introduction

The Massachusetts Institute of Technology Lincoln Laboratory is currently involved in the development of heterodyne detection technology for use on high data rate, intersatellite, optical communication links. As part of this endeavor, we are designing a semiconductor laser transmitter payload to be placed in geosynchronous orbit late in 1989. To lessen the cost and complexity of our initial technology demonstration, the companion heterodyne receiver will be located on earth, with future systems to be entirely space-based.

Atmospheric effects and the resulting degradation in system performance are major considerations in the design of the satellite-to-earth optical communication link. Atmospheric effects at optical and near-optical wavelengths can be divided into three categories: absorption, scattering, and turbulence.¹ Absorption and scattering primarily reduce the amplitude of the received wave front, while turbulence introduces random wave front fluctuations in both amplitude and phase. Reductions in amplitude, due to absorption and scattering, are relatively time-invariant, changing slowly as weather conditions evolve or as clouds pass overhead. They are also nonstatistical in nature. By contrast, turbulence-induced fluctuations are stochastic and can vary at rates as high as a hundred times per second. Although the three atmospheric effects differ considerably, their end result is the same, namely, a degradation in communication link performance.

This degradation is usually characterized as a loss in signal-to-noise ratio.

The portion of this loss attributable to turbulence is stochastic and consequently can only be completely described by its cumulative probability distribution. Most researchers, however, have computed only the mean or variance of the loss,^{2,3} even though these statistics alone are inadequate for predicting communication system performance. A notable exception can be found in the work of Churnside and McIntyre who used an approximate analysis involving Zernike polynomials to derive probability densities.^{4,5} Their technique, however, relies on the implicit assumption that the coefficients in the Zernike polynomial expansions are uncorrelated, and they are not.⁶ In this paper a different approach for calculating the probability density for an optical heterodyne detection system is described. The approach is based on simulation and yields mean and variance values consistent with those obtained using other techniques. The method is illustrated by evaluating the degradation in communication performance on satellite-to-earth and earth-to-satellite links. The calculations are performed for downlinks, with and without angle tracking, and for uplinks, with and without adaptive optics. Heterodyne detection is assumed on all links, and an operating wavelength of $0.84 \mu\text{m}$ is used in the calculations.⁷

This paper is organized as follows. Section II summarizes absorption and scattering effects, information which should prove useful in assessing the relative importance of these phenomena compared with those of turbulence. Section III describes turbulence and its effect on optical heterodyne detection. This discussion closely parallels the work of Fried.² Section IV presents a simulation technique for calculating signal-to-noise ratio probability densities in optical heterodyne detection systems. Section V specifies the near-

The author is with MIT Lincoln Laboratory, P.O. Box 73, Lexington, Massachusetts 02173.

Received 5 September 1985.

0003-6935/86/111817-09\$02.00/0.

© 1986 Optical Society of America.

field phase structure function, a quantity which is needed to perform the simulations described in Sec. IV. The phase structure function is presented for four cases: downlink, downlink with angle tracking, uplink, and uplink with adaptive optics. Section VI contains simulation results for an optical heterodyne detection communication system. Cumulative probability distributions of the received signal-to-noise ratio are given, and the resulting degradation in communication system performance is quantified. Section VII contains our conclusions.

II. Absorption and Scattering

Absorption occurs when the optical electromagnetic field transfers energy to the molecular constituents of the atmosphere.^{8,9} This transfer, which can be described quantum mechanically, results in an increase of the molecules rotational, vibrational, or electronic internal energy. Absorption effects exhibit extreme wavelength dependencies, and in some instances can be mitigated by judiciously choosing the operating wavelength. Figures 1 and 2 show the energy loss due to absorption of an optical beam propagating through the atmosphere from a satellite to a ground station. The ground station is at an altitude of 10,000 ft-above sea level in a tropical environment, and the zenith angle of the satellite is 45°. As Figs. 1 and 2 indicate, absorption losses of <2.4 dB are to be expected between 0.8380 and 0.8500 μm . Clearly, operation between 0.8200 and 0.8380 μm is ill-advised because of the large number of strong absorption lines which occur in this band. The values given in Figs. 1 and 2 were produced using the HITRAN software developed at the U.S. Air Force Geophysical Laboratory.¹⁰

Absorption values are a function of climatological conditions, and thus the data presented in Figs. 1 and 2 are only characteristic of a typical tropical environment without cloud cover. Although absorption values change with climatological conditions, the wavelength locations of the discrete absorption lines do not. In the wavelength region between 0.8 and 0.9 μm , most

absorption is due to atmospheric water vapor content.

Scattering, as opposed to absorption, does not produce a net change in the internal energy states of molecules. It is explained in terms of electromagnetic wave theory and the electron theory of matter.¹¹ Scattering occurs when the optical electromagnetic wave sets in oscillation the electric charges which constitute the scattering particle. This particle can be any bit of matter such as an air molecule or a fog droplet. Scattering losses are not a strong function of wavelength at visible and near visible wavelengths. They are, however, a strong function of visibility conditions. At a wavelength of 0.84 μm , a computer code produced by the U.S. Air Force Geophysics Laboratory¹² indicates that a scattering loss of <1 dB is to be expected on a satellite-to-earth communication link. This 1-dB value assumes that the ground station is at an altitude of 10,000-ft above sea level, the satellite zenith angle is 45°, weather conditions at sea level are clear (i.e., visibility = 20 km), and there is no cloud cover. Optical scattering losses due to even small amounts of cloud cover can be severe (i.e., greater than tens of decibels), thus limiting communications to those time periods when there are no clouds.

III. Turbulence and Optical Heterodyne Detection

Turbulence refers to the time-varying inhomogeneous refractive-index structure of the atmosphere, and it is even present in excellent visibility conditions. The refractive-index inhomogeneity is of the order of one part in a million and is a result of the nonuniform temperature structure of the atmosphere. Turbulence can be modeled qualitatively as if the atmosphere consisted of a set of seak lenses of varying diameters. The atmosphere changes in time as these lenses are moved by the winds. A stationary lens which is larger than the beam diameter will only change the angular orientation (i.e., tilt) of the propagating beam. Thus, the wind-induced motion of large lenses will cause the beam to dance around its nominal arrival angle. Conversely, lenses which are small with

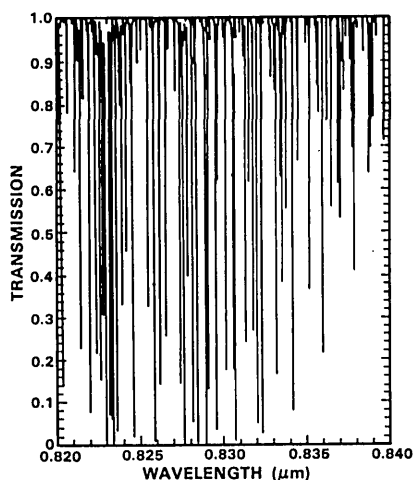


Fig. 1. Absorption spectral line plot (0.82–0.84 μm).

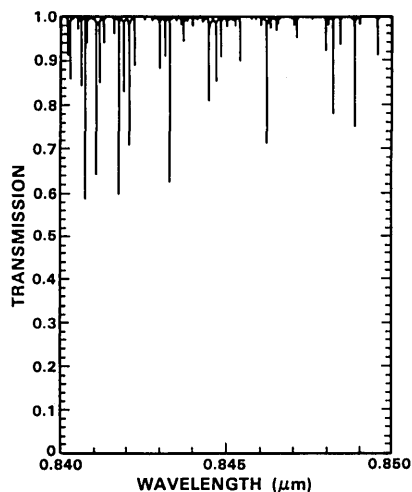


Fig. 2. Absorption spectral line plot (0.84–0.85 μm).

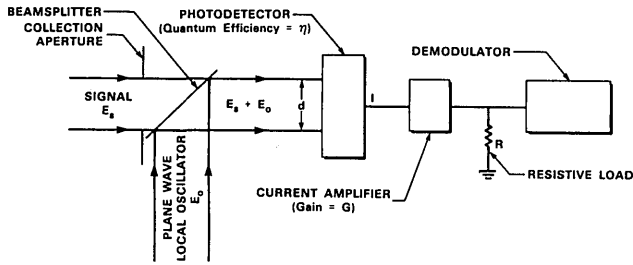


Fig. 3. Optical heterodyne receiver structure.

respect to the beam diameter lead to diffraction effects, and these diffractive effects result in beam broadening and intensity scintillation. The nature of turbulence differs from both absorption and scattering because it has a relatively rapid time-varying characteristic (i.e., up to ≈ 100 Hz) and because it distorts the phase, not just the amplitude, of the received wave front. It is this turbulence-induced phase perturbation which limits the resolution of the best ground-based telescopes, regardless of size, to ~ 1 sec of arc.^{13,14}

Figure 3 illustrates the optical heterodyne receiver structure associated with a communication link from a satellite to a ground station. The receiver structure shown has been simplified for the sake of clarity, and the discussion which follows parallels the work of Fried.² The effect of atmospheric turbulence can be modeled as an amplitude and phase perturbation of the received beam. These perturbations are expressed mathematically by writing the received signal field, $E_s(\mathbf{X})$, as follows:

$$E_s(\mathbf{X}) = A_s(\mathbf{X}) \exp[i\phi(\mathbf{X})] \exp(i2\pi f_s t), \quad (1)$$

where $A_s(\mathbf{X})$, $\phi(\mathbf{X})$, and f_s are the amplitude, phase, and frequency of the field at point \mathbf{X} . We treat the case of frequency modulation for which the signal information is contained in f_s . If the modulation is 8-ary frequency shift keying (FSK), f_s can assume one of eight discrete frequencies. In the absence of turbulence $A_s(\mathbf{X})$ and $\phi(\mathbf{X})$ are constants.

As indicated in Fig. 3, the received signal field is mixed with a plane wave local oscillator field, $E_o(\mathbf{X})$, described by

$$E_o(\mathbf{X}) = A_o \exp(i\phi_o) \exp(i2\pi f_o t). \quad (2)$$

The current I produced by the photodetector is proportional to the power of the incident field integrated over the detector's collection aperture. Thus we can write

$$I = \eta \int W(\mathbf{X}) [E_o(\mathbf{X}) + E_s(\mathbf{X})] [E_o(\mathbf{X}) + E_s(\mathbf{X})]^* d\mathbf{X}, \quad (3)$$

where η = detector quantum efficiency,

$$W(\mathbf{X}) = \begin{cases} 1, & |\mathbf{X}| \leq \frac{d}{2}, \\ 0, & |\mathbf{X}| > \frac{d}{2}, \end{cases} \quad (4)$$

and * denotes complex conjugate. Note that $W(\mathbf{X})$

defines the region of the detector's collection aperture—assumed to be a circle of diameter d . Combining Eqs. (1)–(3) yields

$$I = \eta \int W(\mathbf{X}) A_s^2(\mathbf{X}) d\mathbf{X} + \eta \int W(\mathbf{X}) A_o^2 d\mathbf{X} + \eta \int W(\mathbf{X}) 2A_o A_s(\mathbf{X}) \cos[2\pi(f_s - f_o)t + \phi(\mathbf{X}) - \phi_o] d\mathbf{X}. \quad (5)$$

Since in a well-designed heterodyne detection system the local oscillator power is considerably larger than the received signal power,¹⁵ Eq. (5) can be written as

$$I \approx \eta \int W(\mathbf{X}) A_o^2 d\mathbf{X} + \eta \int W(\mathbf{X}) 2A_o A_s(\mathbf{X}) \cos[2\pi(f_s - f_o)t + \phi(\mathbf{X}) - \phi_o] d\mathbf{X}. \quad (6)$$

The information containing portion of the photocurrent, denoted I_s , is clearly given by

$$I_s = \eta \int W(\mathbf{X}) 2A_o A_s(\mathbf{X}) \cos[2\pi(f_s - f_o)t + \phi(\mathbf{X}) - \phi_o] d\mathbf{X}. \quad (7)$$

Thus the information bearing signal power received by the demodulator, P_s , is given by

$$P_s = \langle (GI_s)^2 R \rangle = 4G^2 R \eta^2 A_o^2 \langle \int W(\mathbf{X}) A_s(\mathbf{X}) \cos[2\pi(f_s - f_o)t + \phi(\mathbf{X}) - \phi_o] d\mathbf{X} \rangle^2, \quad (8)$$

where the brackets $\langle \rangle$ denote a time average. Equation (8) can be written as

$$P_s = 2G^2 R \eta A_o^2 \iint W(\mathbf{X}) W(\mathbf{X}') A_s(\mathbf{X}) A_s(\mathbf{X}') \times \langle \cos[4\pi(f_s - f_o)t + \phi(\mathbf{X}) + \phi(\mathbf{X}') - 2\phi_o] \rangle d\mathbf{X} d\mathbf{X}' + 2G^2 R \eta^2 A_o^2 \iint W(\mathbf{X}) W(\mathbf{X}') A_s(\mathbf{X}) A_s(\mathbf{X}') \times \cos[\phi(\mathbf{X}) - \phi(\mathbf{X}')] d\mathbf{X} d\mathbf{X}' = 2G^2 R \eta^2 A_o^2 \iint W(\mathbf{X}) W(\mathbf{X}') A_s(\mathbf{X}) A_s(\mathbf{X}') \times \cos[\phi(\mathbf{X}) - \phi(\mathbf{X}')] d\mathbf{X} d\mathbf{X}'. \quad (9)$$

In the last step above, the term containing $\cos[4\pi(f_s - f_o)t + \phi(\mathbf{X}) + \phi(\mathbf{X}') - 2\phi_o]$ has been dropped, because it oscillates so rapidly that its time average is zero. Using complex notation, Eq. (9) becomes

$$P_s = 2G^2 R \eta^2 A_o^2 \int W(\mathbf{X}) A_s(\mathbf{X}) \exp[i\phi(\mathbf{X})] d\mathbf{X} \int W(\mathbf{X}') A_s(\mathbf{X}') \exp[-i\phi(\mathbf{X}')] d\mathbf{X}'. \quad (10)$$

If loss ν is defined as the signal power in the presence of turbulence divided by the signal power in the absence of turbulence, it follows from Eq. (10) that

$$\nu \triangleq \text{loss} = \frac{|\int W(\mathbf{X}) A_s(\mathbf{X}) \exp[i\phi(\mathbf{X})] d\mathbf{X}|^2}{A^2 (\int W(\mathbf{X}) d\mathbf{X})^2}, \quad (11)$$

where

$$A_s(\mathbf{X}) = \text{constant} = A \text{ in the absence of turbulence.} \quad (12)$$

Note that the loss in signal-to-noise ratio equals the loss in signal power.

The mean and variance of ν have been calculated analytically by Fried,^{2,3} but there is an error in his variance calculation.¹⁶ The error stems from an approximation made in Sec. III of his paper. Banakh¹⁶ and Massa¹⁷ have performed variance calculations using a Monte Carlo numerical integration technique which avoids Fried's error. It is our goal, however, as stated in Sec. I, to compute the cumulative probability distribution of ν rather than only its first and second moments.

We note that most of the atmospheric turbulence occurs within the first 10 km of the earth's surface.

Thus, for a reasonably sized earth-based collection aperture (i.e., $d > 10$ cm) and for a wavelength of $0.84 \mu\text{m}$, the turbulence is within the near field [i.e., $d > (10^4 \times 0.84 \times 10^{-6})^{1/2} \text{ m}$].

In such a situation, it can be shown that most of the loss in signal-to-noise ratio is due to the phase perturbation $\phi(\mathbf{X})$ rather than the amplitude scintillation $A_s(\mathbf{X})$.¹⁸ Thus, we can write

$$v \simeq \omega^{-1} \left| \int W(\mathbf{X}) \exp[i\phi(\mathbf{X})] d\mathbf{X} \right|^2, \quad (13)$$

where

$$\omega = \left(\int W(\mathbf{X}) d\mathbf{X} \right)^2 = (\text{area of collection aperture})^2. \quad (14)$$

It is not necessary to neglect amplitude scintillation in order to use the simulation technique described in the next section, but it does simplify matters greatly.

IV. Probability Density Calculation

It was shown in the previous section that the loss in signal-to-noise ratio v is given by

$$v \simeq \omega^{-1} \left| \int W(\mathbf{X}) \exp[i\phi(\mathbf{X})] d\mathbf{X} \right|^2, \quad (15)$$

where

$$\omega = \left[\int W(\mathbf{X}) d\mathbf{X} \right]^2 \quad (16)$$

In this section, a simulation technique for calculating the probability distribution of v will be described.

Equation (15) can be written as follows:

$$v \simeq \omega^{-1} \left| \int W(\mathbf{X}) \exp[i\theta(\mathbf{X})] d\mathbf{X} \right|^2, \quad (17)$$

where

$$\theta(\mathbf{X}) \triangleq \phi(\mathbf{X}) - \phi(\mathbf{O}). \quad (18)$$

The phase $\phi(\mathbf{X})$ of the received wave front is a statistical quantity which is both Gaussian and stationary in \mathbf{X} .¹⁹ Thus the quantity $\theta(\mathbf{X})$ is a zero mean, stationary, Gaussian random process, and as such is completely specified by its autocorrelation function $R_\theta(\mathbf{X} - \mathbf{X}')$ defined by

$$R_\theta(\mathbf{X} - \mathbf{X}') \triangleq \overline{\theta(\mathbf{X})\theta(\mathbf{X}')}, \quad (19)$$

where the overbar denotes a statistical average.

Using the algebraic identity

$$(a - b)(c - d) = -\frac{1}{2}(a - c)^2 - \frac{1}{2}(b - d)^2 + \frac{1}{2}(a - d)^2 + \frac{1}{2}(b - c)^2, \quad (20)$$

it follows that

$$\begin{aligned} R_\theta(\mathbf{X} - \mathbf{X}') &= -\frac{1}{2} \overline{[\phi(\mathbf{X}) - \phi(\mathbf{X}')]^2} + \frac{1}{2} \overline{[\phi(\mathbf{X}) - \phi(\mathbf{O})]^2} \\ &\quad + \frac{1}{2} \overline{[\phi(\mathbf{X}') - \phi(\mathbf{O})]^2} \\ &= -\frac{1}{2} D_\phi(\mathbf{X} - \mathbf{X}') + \frac{1}{2} D_\phi(\mathbf{X}') + \frac{1}{2} D_\phi(\mathbf{X}), \end{aligned} \quad (21)$$

where

$$D_\phi(\delta) \triangleq \overline{[\phi(\mathbf{X} + \delta) - \phi(\mathbf{X})]^2}. \quad (22)$$

$D_\phi(\delta)$, which is referred to as the phase structure function in atmospheric optics, will be specified in Sec. V.

For now, however, let us assume that $D_\phi(\delta)$ and hence $R_\theta(\mathbf{X} - \mathbf{X}')$ are known.

The integral in Eq. (15) can be approximated by the following sum:

$$v \simeq \left| \frac{1}{N} \sum_{j=1}^N \exp[i\theta(\mathbf{X}_j)] \right|^2, \quad (23)$$

where the $\mathbf{X}_1, \mathbf{X}_2, \dots, \mathbf{X}_N$ are N sample points within the collection aperture. In Appendix A it is shown that the mean-squared error ϵ that results from approximating the integral of Eq. (17) by this sum is bounded above by

$$\begin{aligned} \epsilon &\leq 4\omega^{-1} \iint W(\mathbf{X})W(\mathbf{Y}) \exp\left[-\frac{1}{2}D_\phi(\mathbf{X} - \mathbf{Y})\right] d\mathbf{X}d\mathbf{Y} \\ &\quad - 8\omega^{-1/2} \frac{1}{N} \sum_{j=1}^N \int \exp\left[-\frac{1}{2}D_\phi(\mathbf{X} - \mathbf{X}_j)\right] d\mathbf{X} \\ &\quad + 4 \frac{1}{N^2} \sum_{j=1}^N \sum_{k=1}^N \exp\left[-\frac{1}{2}D_\phi(\mathbf{X}_j - \mathbf{X}_k)\right]. \end{aligned} \quad (24)$$

Note that the $\theta(\mathbf{X}_1), \dots, \theta(\mathbf{X}_N)$ are zero mean, identically distributed, correlated Gaussian random variables. A method for evaluating v using a computer experiment now becomes apparent. Statistically independent sets of $\theta(\mathbf{X}_1), \dots, \theta(\mathbf{X}_N)$ are generated M times, and for each of these sets v is computed using Eq. (23). The cumulative probability distribution, $P_{\text{cum}}(z)$, defined by

$$P_{\text{cum}}(z) \triangleq \text{probability } v < z, \quad (25)$$

is then approximated as follows:

$$P_{\text{cum}}(z) \simeq \frac{(\text{number of times } v < z)}{M}. \quad (26)$$

The variance of the estimate of $P_{\text{cum}}(z)$ is the variance of a binomial distribution. Thus,

$$\text{variance} = P_{\text{cum}}(z)[1 - P_{\text{cum}}(z)]/M. \quad (27)$$

A technique for generating the correlated Gaussian random variables, $\theta(\mathbf{X}_1), \dots, \theta(\mathbf{X}_N)$, is described next.

There are simple methods available for generating statistically independent Gaussian random variables.²⁰ Let G denote an $N \times 1$ column vector consisting of N , zero mean, unit variance, statistically independent, Gaussian random variables generated by one of these methods. Then we will show that there exists a matrix C such that the matrix product $C \cdot G$ is an $N \times 1$ column vector whose elements are $\theta(\mathbf{X}_1), \dots, \theta(\mathbf{X}_N)$. We note that this method of generating correlated Gaussian random variables is essentially the inverse of the whitening process commonly encountered in statistical communication theory.²¹

Let B denote the $N \times N$ correlation matrix whose j th, k th element b_{jk} (i.e., the element in row j and column k) is defined as

$$b_{jk} \triangleq \overline{\theta(\mathbf{X}_j)\theta(\mathbf{X}_k)} = R_\theta(\mathbf{X}_j - \mathbf{X}_k). \quad (28)$$

Note that the elements of the column vector $C \cdot G$ are Gaussian, because linear transformations preserve Gaussian statistics.²² It is also clear that the elements

of $C \cdot G$ are zero mean. Thus, it is sufficient to find a matrix C which satisfies the following condition:

$$B = \overline{(C \cdot G)(C \cdot G)^t}, \quad (29)$$

where superscript t denotes the matrix transpose. We also note that

$$\overline{(C \cdot G)(C \cdot G)^t} = C \cdot \overline{G \cdot G^t} \cdot C^t = C \cdot C^t. \quad (30)$$

Since B is a correlation matrix it must be real, symmetric, and positive semidefinite.²³ From the real and symmetric property it follows that B has a complete set of N orthonormal eigenvectors, and from the positive semidefinite property it follows that the corresponding eigenvalues must be non-negative.²⁴ Let T denote the matrix whose columns T_j are the orthonormal eigenvectors of matrix B . Let λ_j denote the eigenvalue corresponding to the eigenvector T_j . Then we can write

$$B \cdot T = T \cdot \begin{bmatrix} \lambda_1 & \circ \\ & \lambda_2 \\ \circ & & \lambda_N \end{bmatrix},$$

$$B = T \cdot \begin{bmatrix} \lambda_1 & \circ \\ & \lambda_2 \\ \circ & & \lambda_N \end{bmatrix} \cdot T^t,$$

$$B = T \cdot \begin{bmatrix} \lambda_1^{1/2} & \circ \\ & \lambda_2^{1/2} \\ \circ & & \lambda_N^{1/2} \end{bmatrix} \left(T \cdot \begin{bmatrix} \lambda_1^{1/2} & \circ \\ & \lambda_2^{1/2} \\ \circ & & \lambda_N^{1/2} \end{bmatrix} \right)^t. \quad (31)$$

Comparing Eqs. (29)–(31) yields the following desired result:

$$C = T \cdot \begin{bmatrix} \lambda_1^{1/2} & \circ \\ & \lambda_2^{1/2} \\ \circ & & \lambda_N^{1/2} \end{bmatrix}. \quad (32)$$

Thus, determining the matrix C is equivalent to finding the eigenvalues and eigenvectors of matrix B . The results of Sec. VI are based on a fifty point, $\mathbf{X}_1, \mathbf{X}_2, \dots, \mathbf{X}_N$, sampling of the collection aperture. The correlation matrix B is then evaluated using Eqs. (21), (22), and (28). Finally, the eigenvectors and eigenvalues of the 50×50 matrix B are computed using a scientific software package.

V. Phase Structure Function

In this section the phase structure function, $D_\phi(\delta)$, defined by Eq. (22) is specified. Four cases are considered—downlink, downlink with angle tracking, uplink, and uplink with adaptive optics. $D_\phi(\delta)$ can be calculated using several different methods, all of which are perturbation techniques.¹⁹ These techniques yield approximate solutions to the stochastic electromagnetic wave equation given by

$$\nabla \mathbf{E} + \left(\frac{2\pi}{\lambda} \right)^2 n^2 \mathbf{E} = 0, \quad (33)$$

where \mathbf{E} is the electric field vector, λ is the wavelength, and n is the refractive index of the atmosphere. n is a statistical quantity, and thus Eq. (33) is stochastic. n

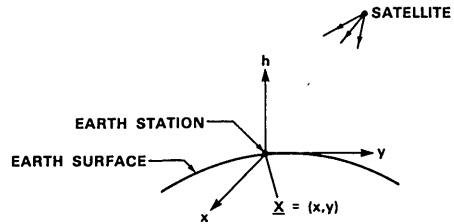


Fig. 4. $h - \mathbf{X}$ coordinate system.

can be written as a function of two variables h and \mathbf{X} which together specify position. The quantities h and \mathbf{X} are defined in Fig. 4. The statistical properties of turbulence have been studied by Kolmogorov,²⁵ and his work along with others has led to the following relationship (Ref. 19, p. 164):

$$\overline{[n(h, \mathbf{X}) - n(h', \mathbf{X}')]^2} = C_n^2 \left(\frac{h + h'}{2} \right) \cdot \|\mathbf{X} - \mathbf{X}'\|^2 + (h - h')^2)^{1/3}, \quad (34)$$

where $C_n^2(\)$, the refractive-index structure parameter, is a measurable quantity which is a function of altitude above the earth's surface. The refractive-index structure parameter changes with time of day, time of year, and with local atmospheric conditions.²⁶ Figure 5 shows two C_n^2 profiles provided by the Rome Air Development Center, and these profiles will be used to generate our results in Sec. VI.

A. Downlink

For the downlink it was first shown by Tatarski¹⁹ that

$$D_\phi(\delta) \triangleq \langle [\phi(\mathbf{X} + \delta) - \phi(\mathbf{X})]^2 \rangle = 2.91(\sec^2 \alpha) |\delta|^{5/3} \int_0^\infty C_n^2(h) dh, \quad (35)$$

where α = zenith angle of the satellite. A simple ray optics derivation of Eq. (35) can also be found in a paper by Fried.²⁷ In the literature, Eq. (35) is often written as

$$D_\phi(\mathbf{X}_1 - \mathbf{X}_2) = 6.88(|\mathbf{X}_1 - \mathbf{X}_2|/r_0)^{5/3}, \quad (36)$$

where

$$r_0 \triangleq \text{transverse coherence length}$$

$$= \left[0.423(\sec^2 \alpha) \left(\frac{2\pi}{\lambda} \right)^2 \int_0^\infty C_n^2(h) dh \right]^{-3/5} \quad (37)$$

Using Eq. (37) and the C_n^2 profiles of Fig. 5, the daytime and nighttime values of r_0 (at $\lambda = 0.84 \mu\text{m}$) are calculated to be 8.9 and 16.4 cm, respectively.

B. Downlink with Angle Tracking

As discussed in Sec. III, turbulent effects can be divided into three categories—angle of arrival fluctuations, beam spreading, and scintillation. A significant portion of the turbulence-induced signal loss in a heterodyne detection system is due to angle of arrival fluctuations alone, and this loss can be removed by tracking the arrival angle of the downlink beam. Because of imperfect orbit prediction capabilities and

because the earth-based antenna gain pattern is extremely narrow, angle tracking is probably required on the downlink even if there is no turbulence. Thus, it is reasonable to determine communication performance in the presence of turbulence assuming downlink angle tracking. The angle-tracked phase structure function, $D_\phi^{AT}(\delta)$, is needed to perform this task. $D_\phi^{AT}(\delta)$ was first calculated (approximately) by Fried, and he obtained the following result¹⁴:

$$D_\phi^{AT}(\delta) \approx 6.88(|\delta|/r_0)^{5/3}[1 - (|\delta|/d)^{1/3}]. \quad (38)$$

Fried's calculation assumed that the phase of the tilt corrected wave front and the tilt component itself were uncorrelated. Although this assumption is not valid, the final result expressed by Eq. (38) remains reasonably accurate. In fact, we have evaluated the angle-tracked phase structure function exactly and have found Eq. (38) to be in error by $<6.88(|\delta|/r_0)^{5/3} 1.5 \times 10^{-2}$.

C. Uplink

Using reciprocity arguments developed by Shapiro²⁸ and by Fried and Yura²⁹ for optical propagation, it can be rigorously shown that uplink and downlink loss statistics will be identical. In this subsection, a simpler, less rigorous approach is used to demonstrate this fact.

The transmitting aperture of a geosynchronous satellite is so far removed from the earth that it appears as a point source when viewed by the receiver on earth. Consequently, the downlink beam is essentially collimated by the time it reaches the atmosphere, and diffraction effects arising from the finite size of the satellite transmitting aperture can be safely neglected. On the uplink a similar situation does not exist, since the atmosphere lies in close proximity to the earth-based transmitter. Thus, the uplink beam will not remain collimated as it propagates through the atmosphere (even in the absence of turbulence) but will experience diffraction because of the finite size of the earth-based transmitting aperture. In our analysis, these uplink diffraction effects will be neglected, which is tantamount to assuming that the atmosphere lies deep in the near field of the earth-based aperture.

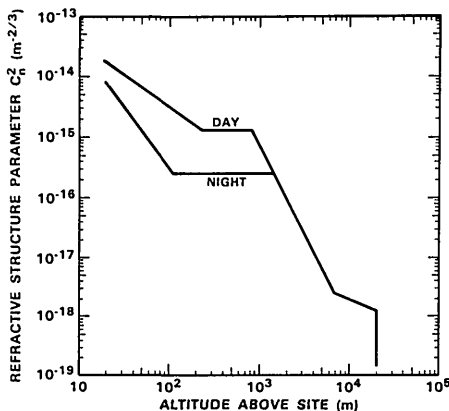


Fig. 5. Refractive-index structure function profiles.

This assumption appears reasonable at a wavelength of $0.84 \mu\text{m}$, provided the diameter of the earth-based aperture exceeds 10 cm. If necessary, the uplink diffraction effects discussed above can be accounted for by using extended Huygens-Fresnel diffraction techniques.³⁰

Since diffraction within the atmosphere is being neglected, ray optics methods are applicable. Using ray optics, it follows that the optical field at the top layer of the atmosphere on the uplink is identical to that which is present at the bottom layer of the atmosphere on the downlink. Thus, Eq. (35) remains a valid description for the uplink phase statistics at the top layer of the atmosphere.

It will be assumed that the distorted wave front at the top layer of the atmosphere lies in the far field of the satellite receiving aperture. This is a reasonable assumption (at a wavelength of $0.84 \mu\text{m}$) for satellites in geosynchronous orbit. In the far field the received electric field $E_u(\mathbf{X}')$ at the satellite will be proportional to the Fourier transform of the field at the top of the atmosphere.³¹ This Fourier transform relationship can be written as follows:

$$E_u(\mathbf{X}) \propto \int W(\mathbf{X}) \exp[i\phi(\mathbf{X})] \exp\left[-i\frac{2\pi}{\lambda L} \mathbf{X} \cdot \mathbf{X}'\right] d\mathbf{X}, \quad (39)$$

where

$$W(\mathbf{X}) = \begin{cases} 1, & \text{inside the earth-based transmitting aperture,} \\ 0, & \text{elsewhere,} \end{cases}$$

L = distance between top of atmosphere and satellite.

For satellites in geosynchronous orbit and for earth-based transmitting and satellite receiving aperture diameters of the order of 20 cm or less, it follows that the term $(\mathbf{X} \cdot \mathbf{X}')/(\lambda L)$ in Eq. (39) is approximately zero. Thus Eq. (39) reduces to

$$E_u(\mathbf{X}') \propto \int W(\mathbf{X}) \exp[i\phi(\mathbf{X})] d\mathbf{X}. \quad (40)$$

The result given by Eq. (40) implies that, unlike the downlink, the optical field received on the uplink is a plane wave.

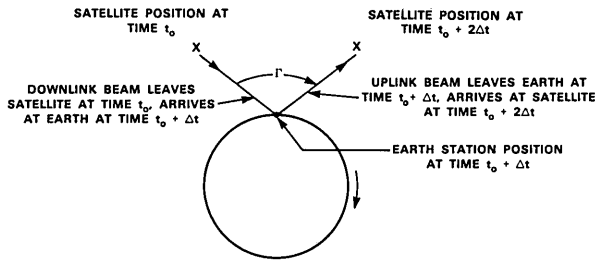
The received signal strength on the uplink is equal to $|E_u(\mathbf{X}')|^2$. Therefore, the turbulence-induced loss on the uplink will be given by

$$\text{loss} = \frac{|\int W(\mathbf{X}) \exp[i\phi(\mathbf{X})] d\mathbf{X}|^2}{|\int W(\mathbf{X}) d\mathbf{X}|^2}. \quad (41)$$

Note that Eq. (41) is identical to Eq. (13), and thus the probability distribution of the signal-to-noise ratio loss is the same for the uplink as for the downlink.

D. Uplink with Adaptive Optics

By sensing the downlink beam from the satellite, the phase perturbation introduced by the turbulent atmosphere can be determined. This information can then be used to predistort the uplink beam (i.e., subtract from it the downlink phase perturbation) before transmission to compensate for the turbulence on the earth-to-satellite uplink. If the uplink and downlink paths were identical, in principle total uplink compensation could be achieved. There are two fundamental factors



$\Delta t = \text{SATELLITE-TO-EARTH PROPAGATION PATH LENGTH/SPEED OF LIGHT}$
 $\Gamma = 2(\text{Angular Rotation Rate of Earth})\Delta t$

Fig. 6. Point-ahead angle.

which preclude total compensation, and they are both related to the finite propagation speed of light. First, atmospheric turbulence is time varying, and thus the atmosphere changes while the downlink beam is traversing it. This effect, however, is rather insignificant, since turbulence changes quite slowly compared to the beam transit time. Second, the satellite moves along its orbit and the earth rotates about its axis while the beam propagates between the earth and the satellite. Therefore, any transmission on either the uplink or downlink must be pointed ahead to reach the moving receiver. This phenomena is analogous to that experienced by a marksman attempting to hit a moving target. The point-ahead effect is illustrated in Fig. 6, from which it can be seen that the uplink and downlink paths are not identical, and thus the possibility of perfect compensation is unrealizable. In fact, for a satellite in a geosynchronous orbit, the uplink and downlink paths can be separated in angle by as much as $21 \mu\text{rad}$ (i.e., $\Gamma = 21 \mu\text{rad}$). For satellites in very low orbits (i.e., 500 km), this value increases to as much as $52 \mu\text{rad}$. The technique of predistorting the transmitted beam to compensate for turbulence is an example of adaptive optics.

The uplink phase structure function, $D_\phi^{AD}(\delta)$, assuming adaptive optics compensation, is given by^{18,32}

$$D_\phi^{AD}(\delta) = 2(2.91)(\sec^2\alpha) \left(\frac{2\pi}{\lambda}\right)^2 \int_0^\infty C_n^2(h) \left[|\delta|^{5/3} + (\Gamma h)^{5/3} - \frac{1}{2}|\delta + \Gamma h(\cos\alpha)e|^{5/3} - \frac{1}{2}|\delta - \Gamma h(\cos\alpha)e|^{5/3} \right] dh, \quad (42)$$

where $\alpha =$ zenith angle of the satellite,
 $\Gamma =$ point-ahead angle, and
 $e =$ a unit vector which lies in the intersection of the plane containing the uplink and downlink paths and the plane tangent to the earth at the ground station location.

A simple and intuitive ray optics derivation of Eq. (42) for $\alpha = 0^\circ$ can be found in Ref. 33.

In this section the phase structure function has been given for four cases of interest—downlink, downlink with angle tracking, uplink, and uplink with adaptive optics. In the next section, these results will be used to determine signal-to-noise ratio probability distributions.

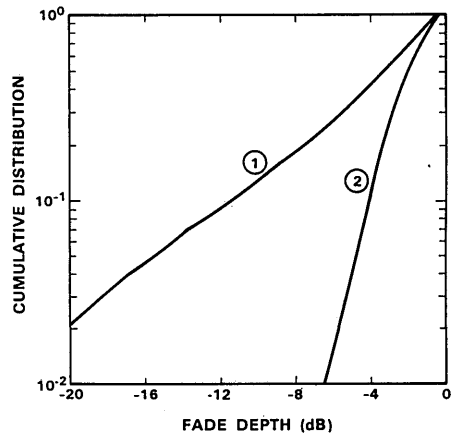


Fig. 7. Fade depth cumulative probability distribution: (1) nighttime uplink or downlink; (2) daytime angle-tracked downlink.

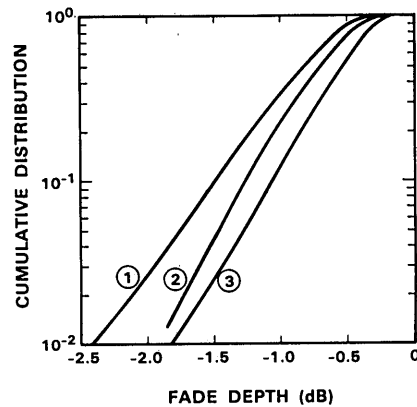


Fig. 8. Fade depth cumulative probability distribution: (1) daytime adaptive optics uplink ($\Gamma = 21 \mu\text{rad}$); (2) nighttime angle-tracked downlink; (3) nighttime adaptive optics uplink.

VI. Results

Cumulative probability distributions for signal-to-noise ratio losses on geosynchronous satellite uplinks and downlinks operating through atmospheric turbulence are given in Figs. 7 and 8. These distributions were calculated using the simulation technique described in Sec. IV with $M = 10,000$ trials. Both the satellite's and the earth terminal's transmit and receive apertures were assumed to have diameters of 16 cm, the operating wavelength was assumed to be $0.84 \mu\text{m}$, and the $C_n^2(h)$ data of Fig. 5 was used.

The degradations in communication system performance, corresponding to the probability distribution of Figs. 7 and 8, were determined for 8-ary, phase incoherent, orthogonal FSK modulation. These degradations are specified quantitatively as follows. First, the signal-to-noise ratio required to support a given channel symbol error rate in the absence of turbulence is computed.³⁴ Next, the signal-to-noise ratio required to maintain that channel symbol error rate in the presence of turbulence is determined using the relationship given by Eq. (43):

$$P_{cs}^{turb} \left(\frac{S}{N} \right) = \int_0^1 P_{cs} \left(v \cdot \frac{S}{N} \right) p(v) dv, \quad (43)$$

where S/N = signal-to-noise ratio,
 $P_{cs}^{turb} (S/N)$ = channel symbol error in the presence of turbulence,
 $P_{cs}(S/N)$ = channel symbol error rate in the absence of turbulence, and
 $p(v)$ = probability density of the signal-to-noise ratio loss v due to turbulence.

Finally, the degradation is computed as the difference between the above two signal-to-noise ratios. We have chosen to specify the degradation at an 8-ary channel symbol error rate of 1.5%. If rate 1/2, constraint length 7, convolutional encoding is used in conjunction with 8-ary FSK modulation, the 1.5% channel symbol error rate corresponds to approximately a 2×10^{-7} hard decision, Viterbi decoded, user bit error rate.

Table I gives the turbulence-induced degradations in communication performance at a 1.5% 8-ary channel symbol error rate for downlinks, with and without angle tracking, and for uplinks, with and without adaptive optics. Also indicated in this table is the mean loss in signal-to-noise ratio defined as

$$\text{mean loss} = \int_0^1 v p(v) dv. \quad (44)$$

We note that the mean loss can be a very poor indicator of the actual degradation in communication system performance. Downlink and uplink losses occurring during the day will exceed those occurring at night, because daytime r_0 values are smaller. Since the nighttime downlink and uplink loss values are already too large to be of practical interest (i.e., 13.3 dB), the two corresponding daytime values were not computed in Table I.

VII. Conclusions

In this paper the three basic atmospheric effects, absorption, scattering, and turbulence, were reviewed. A simulation approach was then developed to determine signal fade probability distributions on heterodyne detected satellite links which operate through atmospheric turbulence. The calculations were performed on both angle-tracked and nonangle-tracked downlinks and on uplinks, with and without adaptive optics. The turbulence-induced degradations in communication performance were determined using signal fade probability distributions, and it was shown that the average signal fade can be a poor measure of the performance degradation.

The author gratefully acknowledges several informal discussions with J. H. Shapiro of MIT concerning the work reported here. The author would also like to express his thanks to Steve Tirrell of Lincoln Laboratory for providing the data shown in Figs. 1 and 2.

This work was sponsored by the Department of the Air Force. The views expressed are those of the author and do not reflect the official policy or position of the U.S. Government.

Table I. Degradation in 8-ary FSK Communication Performance:
¹ Actual Loss; ² Mean Loss

	Daytime (dB)	Nighttime (dB)
Downlink	>13.3 ¹ (7.8) ²	13.3 (3.5)
Angle-tracked downlink	3.3 (2.4)	0.9 (0.8)
Uplink	>13.3 (7.8)	13.3 (3.5)
Adaptive optics uplink	1.1 (1.0)	0.7 (0.7)

Receive and transmit aperture diameters = 16 cm.
 Uplink point-ahead angle $\Gamma = 21 \mu\text{rad}$ (geosynchronous altitude).
 Satellite zenith angle = 90° .
 C_n^2 profile used is given in Fig. 5.

Appendix A: Mean-Squared Error Derivation

$$\mathbf{U} \triangleq \omega^{-1/2} \int W(\mathbf{X}) \exp[i\phi(\mathbf{X})] d\mathbf{X}, \quad (A1)$$

$$\mathbf{Q} \triangleq \frac{1}{N} \sum_{j=1}^N \exp[i\phi(\mathbf{X}_j)]. \quad (A2)$$

Note that $|\mathbf{U}| \leq 1$ and $|\mathbf{Q}| \leq 1$.

$$\begin{aligned} \epsilon \triangleq \text{mean-squared error} &= \frac{(|\mathbf{U}|^2 - |\mathbf{Q}|^2)^2}{(|\mathbf{U}| - |\mathbf{Q}|)^2 (|\mathbf{U}| + |\mathbf{Q}|)^2} \\ &\leq 4 \frac{(|\mathbf{U}| - |\mathbf{Q}|)^2}{|\mathbf{U} - \mathbf{Q}|^2} \\ &\leq 4 \frac{|\mathbf{U} - \mathbf{Q}|^2}{|\mathbf{U} - \mathbf{Q}|^2}, \end{aligned} \quad (A3)$$

$$\mathbf{U} - \mathbf{Q} = \omega^{-1/2} \frac{1}{N} \sum_{j=1}^N \int W(\mathbf{X}) \{\exp[i\phi(\mathbf{X})] - \exp[i\phi(\mathbf{X}_j)]\} d\mathbf{X}, \quad (A4)$$

$$\begin{aligned} |\mathbf{U} - \mathbf{Q}|^2 &= \omega^{-1} \frac{1}{N^2} \sum_{j=1}^N \sum_{k=1}^N \iint W(\mathbf{X}) W(\mathbf{Y}) \{\exp[i\phi(\mathbf{X}) - i\phi(\mathbf{Y})] \\ &\quad - \exp[i\phi(\mathbf{X}) - i\phi(\mathbf{X}_j)] - \exp[i\phi(\mathbf{X}_k) - i\phi(\mathbf{Y})] \\ &\quad + \exp[i\phi(\mathbf{X}_k) - i\phi(\mathbf{X}_j)]\} d\mathbf{X} d\mathbf{Y}. \end{aligned} \quad (A5)$$

Note that

$$\overline{\exp(ia)} = \exp\left(-\frac{1}{2} a^2\right), \quad (A6)$$

for a = any zero mean Gaussian random variable. Thus,

$$\begin{aligned} \epsilon \leq 4|\mathbf{U} - \mathbf{Q}|^2 &= 4\omega^{-1} \iint W(\mathbf{X}) W(\mathbf{Y}) \exp\left[-\frac{1}{2} D_\phi(\mathbf{X} - \mathbf{Y})\right] d\mathbf{X} d\mathbf{Y} \\ &\quad - 8\omega^{-1/2} \frac{1}{N} \sum_{j=1}^N \int W(\mathbf{X}) \exp\left[-\frac{1}{2} D_\phi(\mathbf{X} - \mathbf{X}_j)\right] d\mathbf{X} \\ &\quad + 4 \frac{1}{N^2} \sum_{j=1}^N \sum_{k=1}^N \exp\left[-\frac{1}{2} D_\phi(\mathbf{X}_j - \mathbf{X}_k)\right]. \end{aligned} \quad (A7)$$

References

1. J. W. Strohbehn, "Introduction," in *Laser Beam Propagation in the Atmosphere*, J. W. Strohbehn, Ed. (Springer-Verlag, New York, 1978), pp. 1-7.

2. D. L. Fried, "Optical Heterodyne Detection of an Atmospherically Distorted Signal Wave Front," *Proc. IEEE* **55**, 57 (1967).
3. D. L. Fried, "Atmospheric Modulation Noise in an Optical Heterodyne Receiver," *IEEE J. Quantum Electron.* **QE-3**, 213 (1967).
4. J. H. Churnside and C. M. McIntyre, "Signal Current Probability Distribution for Optical Heterodyne Receivers in the Turbulent Atmosphere. 1: Theory," *Appl. Opt.* **17**, 2141 (1978).
5. J. H. Churnside and C. M. McIntyre, "Signal Current Probability Distribution for Optical Heterodyne Receivers in the Turbulent Atmosphere. 2: Experiment," *Appl. Opt.* **17**, 2148 (1978).
6. R. J. Noll, "Zernike Polynomials and Atmospheric Turbulence," *J. Opt. Soc. Am.* **66**, 207 (1976).
7. J. E. Kaufmann and L. L. Jeromin, "Optical Heterodyne Intersatellite Links Using Semiconductor Lasers," in *IEEE GLOBECOM '84*, Convention Record, Atlanta, GA (26-29 Nov. 1984).
8. E. J. McCartney, *Absorption and Emission by Atmospheric Gases* (Wiley, New York, 1983), Chap. 1.
9. R. K. Long, "Atmospheric Absorption and Laser Radiation," Bulletin 199 (Engineering Experiment Station, Ohio State U., Columbus, OH).
10. L. S. Rothman, "High Resolution Atmospheric Transmittance Radiance: HITRAN and the Data Compilation," *Proc. Soc. Photo-Opt. Instrum. Eng.* **142**, 2 (1978).
11. E. J. McCartney, *Optics of the Atmosphere* (Wiley, New York, 1976), pp. 20-26.
12. F. X. Kneizys *et al.*, "Atmospheric Transmittance/Radiance: Computer Code LOWTRAN 5," AFGL Report AFGL-TR-80-0067 (Air Force Geophysics Laboratory, Lexington, MA, 1980), AD No. A088215.
13. L. W. Fredrick and R. H. Baker, *Astronomy* (Van Nostrand, New York, 1976), p. 85.
14. D. L. Fried, "Optical Resolution Through a Randomly Inhomogeneous Medium for Very Long and Very Short Exposures," *J. Opt. Soc. Am.* **56**, 1372 (1966).
15. R. M. Gagliardi and S. Karp, *Optical Communications* (Wiley, New York, 1976), Chap. 6.
16. V. A. Banakh, G. M. Krekov, V. L. Mironov, S. S. Khmelevtsov, and R. Sh. Tsvik, "Focused-Laser Beam Scintillations in the Turbulent Atmosphere," *J. Opt. Soc. Am.* **64**, 516 (1974).
17. G. P. Massa, "Fourth-Order Moments of an Optical Field that has Propagated Through the Clear Turbulent Atmosphere," M.S. Thesis, Massachusetts Institute of Technology, Cambridge, MA (1975).
18. D. L. Fried, "Anisoplanatism in Adaptive Optics," *J. Opt. Soc. Am.* **72**, 52 (1982).
19. V. I. Tatarski, *Wave Propagation in a Turbulent Medium* (McGraw-Hill, New York, 1961).
20. M. Zelen and N. C. Severo, "Probability Functions," in *Handbook of Mathematical Functions*, M. Abramowitz and I. Stegun, Eds. (Dover, New York, 1965), Chap. 26.
21. I. Selin, *Detection Theory* (Princeton U.P., Princeton, NJ, 1965), pp. 23-28.
22. W. B. Davenport, Jr., *Probability and Random Processes* (McGraw-Hill, New York, 1970), pp. 504-505.
23. W. Feller, *An Introduction to Probability Theory and Its Applications* (Wiley, New York, 1966), Vol. 2, pp. 80-82.
24. F. E. Hohn, *Introduction to Linear Algebra* (Macmillan, New York, 1972), Chap. 9.
25. A. Kolmogorov, "Turbulence," in *Classic Papers in Statistical Theory* S. K. Friedlander and L. Topper, Eds. (Interscience, New York, 1961), pp. 151-155.
26. D. L. Walters, "Atmospheric Modulation Transfer Function for Desert and Mountain Locations: r_0 Measurements," *J. Opt. Soc. Am.* **71**, 406 (1981).
27. D. L. Fried, "Diffusion Analysis for the Propagation of Mutual Coherence," *J. Opt. Soc. Am.* **58**, 961 (1968).
28. J. H. Shapiro, "Reciprocity of the Turbulent Atmosphere," *J. Opt. Soc. Am.* **61**, 492 (1971).
29. D. L. Fried and H. T. Yura, "Telescope-Performance Reciprocity for Propagation in a Turbulent Medium," *J. Opt. Soc. Am.* **62**, 600 (1972).
30. R. F. Lutomirski and H. T. Yura, "Propagation of a Finite Optical Beam in an Inhomogeneous Medium," *Appl. Opt.* **10**, 1652 (1971).
31. J. W. Goodman, *Introduction to Fourier Optics* (McGraw-Hill, New York, 1968), pp. 57-62.
32. G. A. Tyler, "Turbulence-Induced Adaptive-Optics Performance Degradation: Evaluation in the Time Domain," *J. Opt. Soc. Am. A* **1**, 251 (1984).
33. K. A. Winick, "Signal Fade Probability Distributions for Optical Heterodyne Receivers on Atmospherically Distorted Satellite Links," in *IEEE GLOBECOM '84* Convention Record, Atlanta, GA (26-29 Nov. 1984).
34. W. C. Lindsey and M. K. Simon, *Telecommunication Systems Engineering* (Prentice-Hall, Englewood Cliffs, NJ, 1973), pp. 483-499.